Journal of
Composites Science

MDPI

Article

Physico-Chemical, Rheological, and Viscoelastic Properties of Starch Bio-Based Materials

Mohamed Ragoubi *, Caroline Terrié and Nathalie Leblanc

UniLaSalle, Univ. Artois, ULR7519-Transformations & Agro-Ressources, F-76130 Mont Saint Aignan, France
* Correspondence: mohamed.ragoubi@unilasalle.fr

Abstract: This study describes the elaboration and characterization of plasticized starch composites based on lignocellulosic fibers. The transformation of native to plasticized starch (TPS) and the preparation of TPS blends were performed with a new lab-scale mixer based on an original concept. Firstly, the morphology and chemical composition of flax shives were analyzed to better understand the intrinsic properties of these natural fillers. Then, the impact of the processing parameters (temperature, speed screw) on the quality and the structural properties of plasticized starch were examined by SEM and DRX. After that, we focused on the elaboration of various formulations based on plasticized starch matrix by varying TPS formulation and filler content (from 10 to 30%). The viscoelastic and rheological properties of TPS/flax blends have been analyzed by TGA, SEM, and DMTA.

Keywords: starch biopolymer; lignocellulosic flax; extrusion; RMX process; rheological and microstructural properties

Citation: Ragoubi, M.; Terrié, C.; Leblanc, N. Physico-Chemical, Rheological, and Viscoelastic Properties of Starch Bio-Based Materials. *J. Compos. Sci.* **2022**, *6*, 375. https://doi.org/10.3390/jcs6120375

Academic Editor: Francesco Tornabene

Received: 18 October 2022
Accepted: 30 November 2022
Published: 6 December 2022

1. Introduction

Due to environmental concerns and the scarcity of fossil resources, particular interest has been devoted to biobased and biodegradable materials given their multiple advantages over conventional composites [1,2]. This growing interest considers their abundance, low cost, low density and ecological benefits. In particular, natural and biodegradable resources are of interest for the production of biodegradable plastics [3,4]. Among the biodegradable plastics currently on the market, starches and their derivatives (Mater bi, etc.) are gaining attention as raw materials in the production of biodegradable plastics. Several studies have been conducted based on natural green polymers, e.g., starch-based plastics [5–9]. Starch is widely produced throughout the world and is considered a low-cost source. However, its application is limited due to several limitations, including poor processability and low moisture resistance [10,11]. To overcome these issues, different thermomechanical energy and plasticizers such as glycerol [12,13], citric acid [13], sorbitol [14], and soybean oil [15] can be used to convert it to a thermoplastic starch (TPS) that can be extruded or injected. These plasticizers reduce the intermolecular force between starch molecules, improving their mobility.

However, plasticized starch exhibits poor mechanical properties and very brittle behavior resulting from rapid retrogradation [16–18]. Nevertheless, the brittle behavior of TPS can be converted into ductile behavior, with the development of suitable formulations and the understanding of their thermomechanical and rheological properties. Indeed, several authors have recommended the association of starch with other compounds in order to improve the performance of the final product. Dammak et al. [19] and Palai et al. [20] highlighted that coupling agent contributes effectively to improve the interfacial adhesion of TPS to other polymers and consequently their mechanical behavior.

Although, it was reported that the inclusion of nanofillers to TPS phase might be a suitable alternative to overcome their weakness behavior (mechanical and water sensitivity)

without compromising its biodegradability. Dang et al. [21] reported the development of a TPS/PBAT nano-biocomposite using sepiolite nanoclay. These nanoclays improved the dynamic mechanical and water uptake properties of TPS nano-biocomposites. In another research study, the same group prepared a nano-biocomposite by inclusion of halloysite clay nanotubes (HNTs) in the TPS phase. The addition of 5 wt% of HNTs had a notable effect on both tensile strength and Young's modulus. Furthermore, the formulation and characterization of TPS loaded with cellulosic fibers has been studied [22–25] and most authors have found marked improvements in the properties (tensile and impact resistance test) of TPS products. Curvelo et al. [25] used short cellulosic fibers from Eucalyptus pulp as reinforcement for thermoplastic starch. The TPS composite showed an increase in 100% in tensile strength and more than 50% in modulus with respect to non-reinforced thermoplastic starch.

Despite these efforts, the performance of TPS-based materials remains poor and requires further optimization for the design of high-performance biocomposite materials. However, the development of starch-based materials often comes up against the difficulty of effectively dispersing the various constituents of a multiphase system. This situation corresponds to powerful differences in density between the two constituents and the thermal and rheological properties of starch. To overcome these problems, devices other than conventional mixers (single-screw or twin-screw extruders) have recently been described in the literature [26,27]. Their principle favors elongational flow and strongly contributes to increasing the efficiency of the dispersion mechanisms.

This study describes the development of biocomposites based on starch and lignocellulosic aggregates using a new RMX mixer (Elongational flow Reactor and MiXer, SCAMEX, France, Crosne). This device is based on an original concept consisting of mixing the material continuously in a very tight system. Compared with existing laboratory mixers, the flow in the mixture is characterized by a strong contribution from the elongated flows and the ability to directly measure the evolution of the rheological properties of the mixtures. First of all, an understanding of the intrinsic properties of natural flax shives in terms of morphological and biochemical character was necessary. After that, the impact of the process parameters (temperature and screw speed) on the processability of the different formulations were examined.

Then, we developed different biocomposite TPS/flax shives mixtures and examined the evolution of their physico-chemical, rheological, and thermomechanical properties.

2. Materials and Methods

Wheat starch was supplied by Roquette (France, Lestrem). In terms of mass composition and depending on the supplier, starch consists of 25% amylose, 74.8% amylopectin, and 0.2% protein.

Glycerol (>98% purity—Sigma-Aldrich), was also used as a plasticizer. It is incorporated up to 20% by mass in all the formulations. Several authors have shown that 20% glycerol is the optimal level that can act as a plasticizer in starch [28–30].

Linseed shives supplied by Terre de Lin (France, Saint Pierre Le Viger) were also used for the formulation of biocomposite mixtures. These vegetable reinforcements (Figure 1) were ground (RETSH SM100 device, 4 mm grid) and sieved (RETSH, sieve diameter 0.7 and 1 mm) to obtain very homogeneous fractions (diameter between 0.7 and 1 mm).

Figure 1. Crushed and sifted flax shives.

2.1. Description of the Reactor-MiXer (RMX) Process

The RMX process, developed by the company Scamex, is an original concept for mixing multiphase products. This device can also promote chemical reactions evolving towards high viscosities, including the presence of very volatile reagents, and therefore operate as a polymerization reactor. Its principle (Figure 2) is based on alternating flow of liquids, mixed through a static mixing element [31]. As shown in Figure 2, a mixing unit consists of an extrusion screw (L/d = 300/20), two cylindrical chambers (Φ = 32 mm) separated by the static mixing element (L = 20 mm, Φ = 3 mm). Two pistons push (hydraulically) the material alternately from chamber to chamber through the mixing element. The operating conditions are then defined by the number of cycles (piston back and forth), the pressure exerted by the pistons on the material in the chambers, and the diameter of the material outlet.

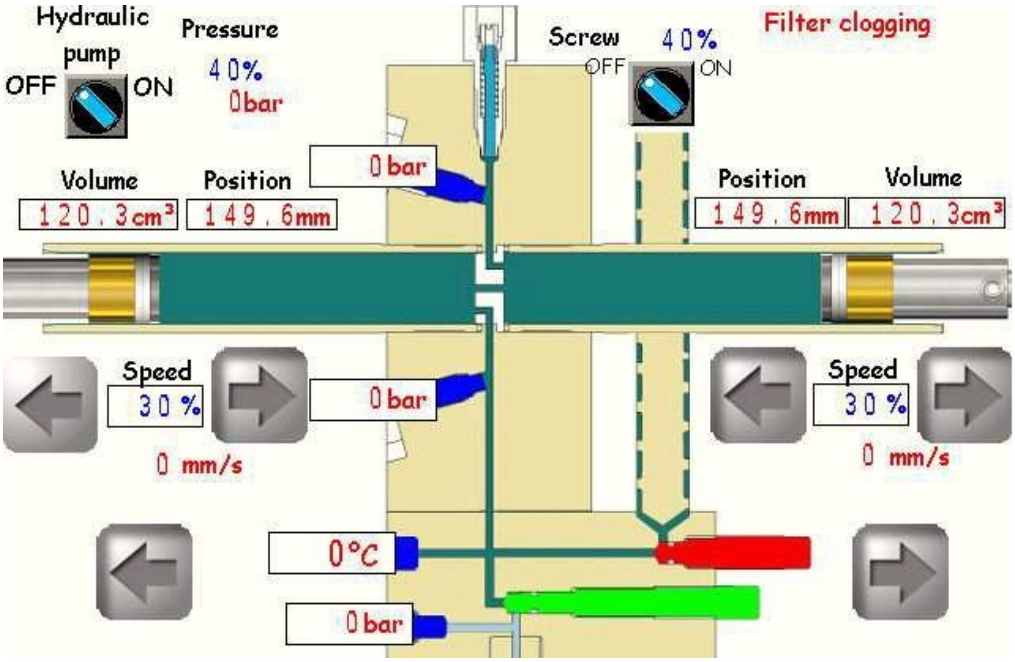

Figure 2. Shematic principle of RMX [31].

2.2. Preparation of Plasticized Starch/Flax Shives Mixtures

First, the starch is plasticized with glycerol (20% by mass) using a turbo-mixer at room temperature. The starch/glycerol mixture is stirred at high speed (1000 rpm) to obtain a homogeneous dispersion. At the end of this step, the resulting mixture is heated up to 170 °C for 45 min to facilitate the diffusion of glycerol into the starch granules and improve its plasticization. Secondly, the plasticized starch is extruded (100 °C at 50 rpm) through a single screw extruder (L/D = 250/32) and granulated. In a third step, the plasticized starch granules are mixed with different fractions of flax shives (10, 15, 20 and 30%) in the RMX mixer (cycle number = 5 and piston speed = 50%). The extrudate obtained is molded directly and thermo-compressed in a hot plate press (200 bars, at 100 °C for 10 min).

2.3. Scanning Elecron Microscopy

SEM analysis was performed with a JEOL-JSM100 Scanning Electron Microscope. The tests were conducted under 15 kV with magnification ranging from ×37 to ×200. No coating was applied to either material. Three specimens, placed on a carbon adhesive tape, were analyzed.

2.4. Chemical Composition

Chemical composition of flax shives, content of ash, lignin, cellulose, hemicellulose, and soluble compounds in neutral detergent was determined following the Van Soest method [27] employing an adapted machine (FibertcTR 8000, Foss). To carry out this measurement all samples were previously dried until constant weight at 40 °C using an oven (Memmert, Germany). All measurements were carried out at least in triplicate.

2.5. X-ray Diffraction Analysis

The analyses were carried out at the SMS Laboratory (University of Rouen) using a D8 diffractometer from Bruker (Germany), equipped with a monochromatic radiation source (λ = 1.541 Å). The experiments were carried out over an angular range 2q from 10° to 50°, in steps of 0.05° with a scanning speed of 0.5°/s. Two specimens were tested for each type of material.

2.6. Thermogravimetric Analysis

Thermogravimetric analysis (TGA) consists of measuring the variation in the mass of a sample as a function of temperature. The measurements were carried out on a NETZCH TG209 thermobalance. The samples of 10 to 15 mg were placed in an alumina crucible and the temperature varied from 25 to 800 °C at a rate of 10 °C/min, under an inert atmosphere (argon) with a start of 20 mL/min. Three specimens were tested for each type of material.

2.7. Thermomechanical Analysis

The viscoelastic properties, namely the modulus of storage, E', the modulus of loss E'', and the mechanical loss factor tan $\delta = E''/E'$, were characterized as a function of temperature. For this, the DMA analysis was performed with Netzsch equipment (DMA 242) at IFTS (University of Reims). Rectangular specimens ($60 \times 10 \times 4$ mm^3) were fixed on a Dual cantilever assembly. The temperature of the analysis varied from 25 to 110 °C, at a heating rate of 3 °C/min. The amplitude and frequency were set at 7.5 and 1 Hz, respectively. Three specimens were tested for each type of material.

3. Results and Discussion

3.1. Morphological Aspect of Flax Shives

From a microstructural scale, flax shives show a cellular structure with a diameter ranging from 10 to 28 µm as shown by MEB analysis (Figure 3). From a macro scale, samples show a regular size distrubution ranging from 0.8 to 1mm, according to the particle size analyzer (not presented here).

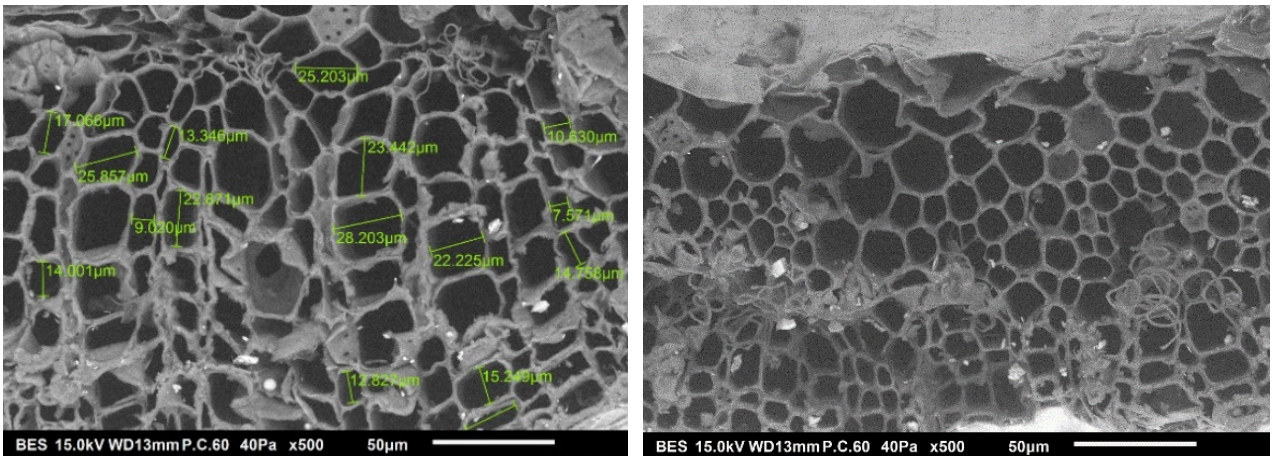

Figure 3. SEM picture of flax shives showing a cellular morphology.

In terms of chemical composition, Table 1 presents the chemical composition of flax shive particles, which is quite similar to reported results in literature [32,33]. We notice mainly the presence of cellulose, lignin, hemicellulose, soluble, and ash fractions.

Table 1. Chemical composition of flax shives.

	Soluble (% d. b.)	**Hemicellulose (% d.b.)**	**Cellulose (% d.b.)**	**Lignin (% d.b.)**	**Ash (% d.b.)**
Chemical composition	8.2 ± 1.4	19.7 ± 1.6	40.2 ± 1.9	27.7 ± 2.1	4.2 ± 0.9

Furthermore, we pushed the chemical study to an Infrared analysis (FTIR) in order to identifiy the different chemical links. From the FTIR spectrogram (Figure 4), we observe:

- The peak at 3347 cm^{-1} corresponds to the O-H group whose characteristic vibration is the elongation of the hydrogen bond of the hydroxyl group in polysaccharides;
- The peaks at (2917 cm^{-1}, 2850 cm^{-1}) are suitable for the C-H bond in the characteristic vibration is the elongation of CH and CH_2 in cellulose and hemicellulose;
- A low intensity peak at around 1500 cm^{-1} is associated with the C=C bond which corresponds to the elongation of the aromatic ring in lignin;
- The peak around 1240 cm^{-1} is due to the stretching vibration of the C-O bonds of the acetyl group in the lignin. The intense peak at 1033 cm^{-1} can be attributed to the elongation vibration C-O and O-H which belong to polysaccharide in cellulose.

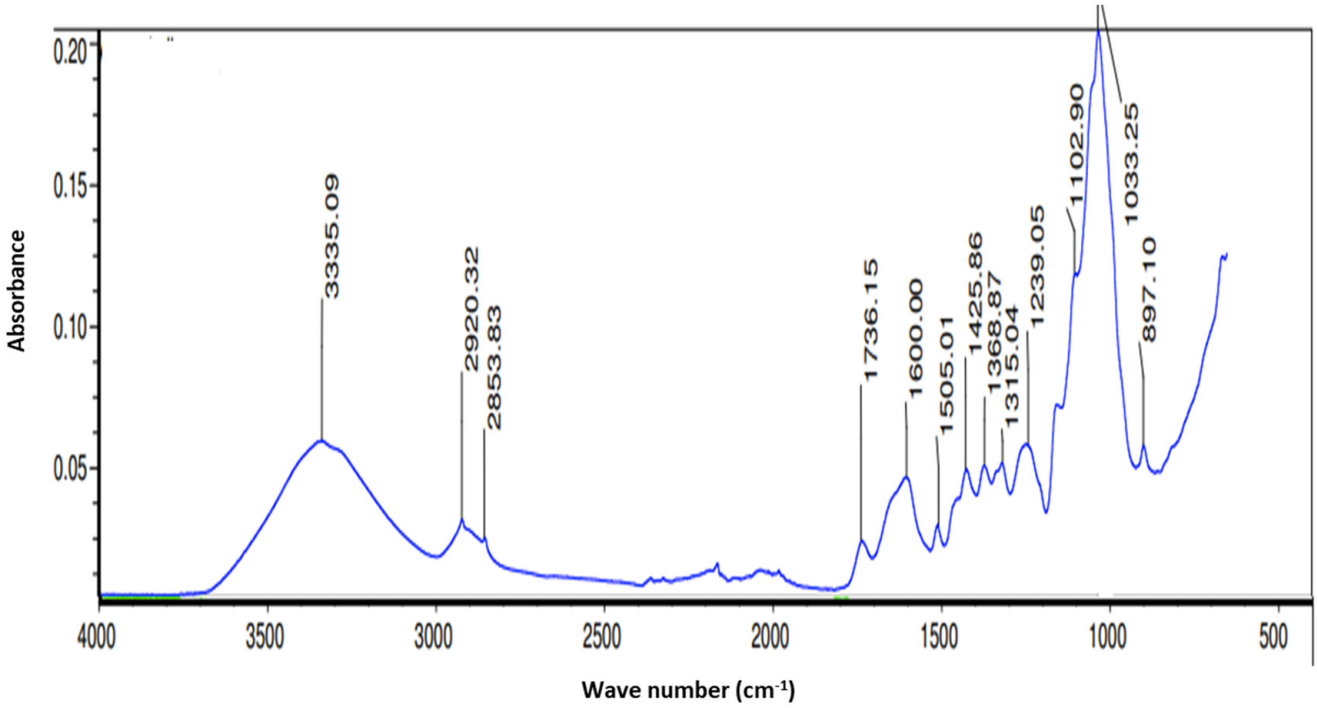

Figure 4. FTIR spectogram of flax shives coproducts.

3.2. Processability of Starch-Based Mixtures in RMX

The TPS/flax shive biocomposite blends were prepared by RMX and several parameters, including temperature and extrusion screw speed, were optimized to facilitate the processability of starch products. For this, the pressure of the hydraulic pump and the speed of the extrusion screw were kept at 100% and 50% of their maximum power, respectively.

For temperatures ranging from 100 to 130 °C, it has been found to be almost impossible to entrain material through the extrusion screw into the mixing chamber. Under these conditions, the TPS granules remain almost intact, and no sign of material softening is observed (the granules become stuck in the feed zone). Beyond 135 °C, the material begins, very slowly, to soften and it shows good processability at 145 °C (fusion zone and compression zone). At this temperature, the TPS obtained appears very clear and transparent (Figure 5a). Above 145 °C, TPS shows good processability and becomes increasingly brownish, a sign of thermal degradation of the starch (Figure 5b).

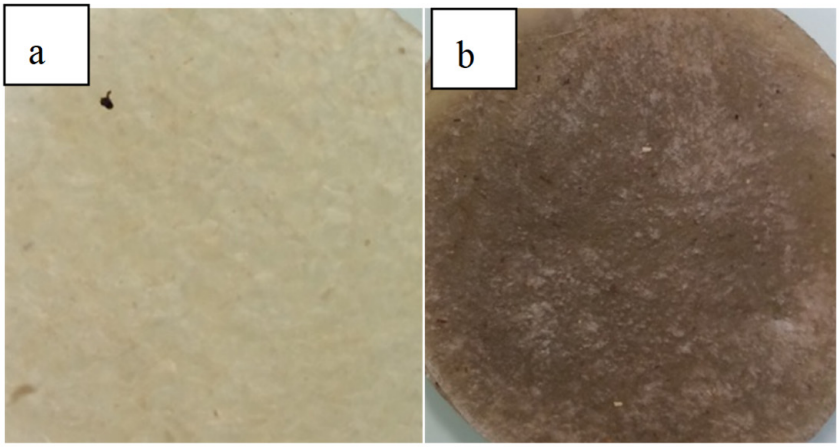

Figure 5. Visual appearance of the plasticized starch (TPS) obtained by RMX: (**a**) 145 °C, (**b**) 160 °C.

Regarding the speed of the extrusion screw (Table 2), the speed range was varied from 50 to 100%. It should be mentioned that for a speed lower than 50%, the torque supplied does not allow material to be driven, whereas, for a speed of 50 to 80%, the material is driven to the mixing chamber without any particular problem. Above 80%, the drive torque reaches its operating threshold and causes the RMX stop.

Table 2. Mixture processability parameters starch-based materials in the RMX.

Parameters	Process Conditions	Optimized Parameters
Temperature	>145 °C	145 °C
Screw speed	50 to 80%	50%

In conclusion, and for the rest of our work, we chose to use an extrusion screw speed set at 50% and a temperature of 145 °C, for the formulation of starch-based mixtures.

3.3. Evolution of the Rheology of Bio-Based Mixtures

The rheological properties of starch-based mixtures are greatly influenced by several factors (temperature, humidity, shear rate, etc.). Using the RMX Reactor-Mixer, it is possible to measure the apparent viscosity of molten mixtures. Indeed, from the measured pressures and the flow rate of the material, it is possible to measure:

$$\text{The apparent viscosity } \eta_{app} = \tau_{app}/\gamma_{app},$$

$$\text{The shear rate } \gamma_{app} = 4\,Q/\pi r^3$$

$$\text{The shear stress: } \tau_{app} = r\,\Delta P/2L$$

where Q is the volume flow rate of the material, P the pressure variation between the two mixing compartments, L the length of the mixing element, and r the radius of the mixing element.

3.3.1. Effect of Cycle Number

Figure 6 shows the variation in the apparent viscosity of plasticized starch as a function of the number of mixing cycles. It should be mentioned that the measurement of this characteristic was carried out at 145 °C while keeping the other parameters constant: pump pressure = 100%, screw extrusion speed = 50%, piston speed = 20 mm/s.

From this graph we observe that after the first two cycles, the apparent viscosity of the TPS is very high. Beyond two mixing cycles, the apparent viscosity tends to gradually decrease, and the mixture becomes more fluid and homogeneous. These observations are all the more confirmed when the flax shives are added in different proportions (10 to 40%). The higher the fiber content, the greater the viscosity. It is also noted that the more the number of mixing cycles increases, the more the viscosity tends to decrease and stabilize after six mixing cycles. This tendency is probably due to a reorganization of the macromolecular chains in situ, generated by the elongational shear and which would also lead to better dispersion of the flax byproducts.

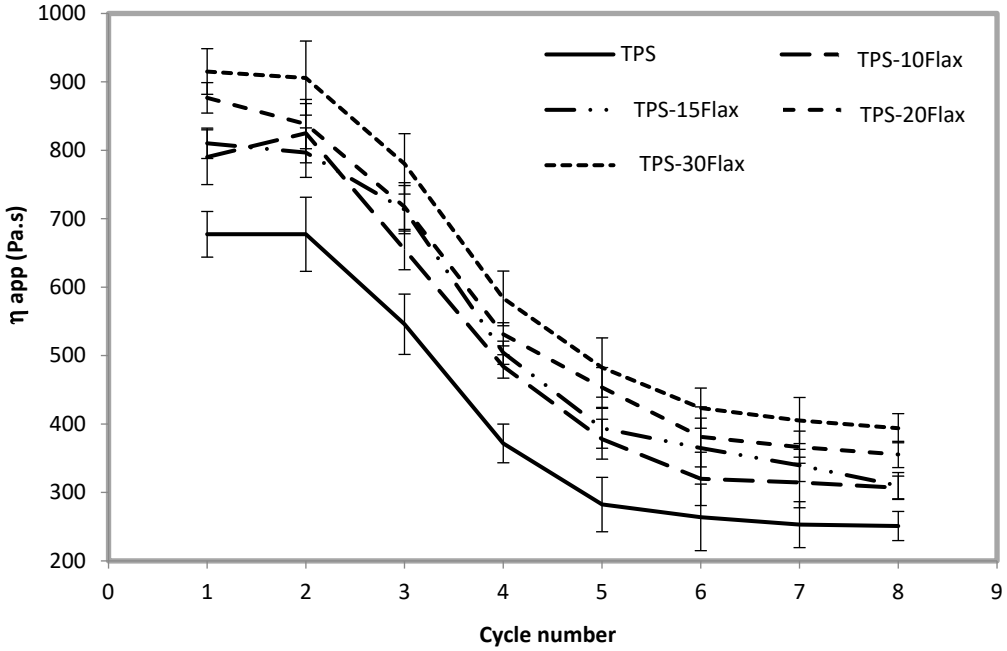

Figure 6. Variation in the apparent viscosity of the TPS mixtures (% percentage) flax shives as a function of the number of cycles (temperature 145 °C).

3.3.2. Effect of Shear Rate

Figure 7 shows the effect of shear rate on the viscosity of starch-based blends. Note that at low speed (<40%) the mixtures are very viscous. The higher the content of flax byproducts, the higher the viscosity [4]. Beyond 40%, the viscosity of the mixtures decreases considerably, which reflects good homogeneity, better dispersion of flax shives and probably good reorientation of the macromolecular chains. However, the addition of flax byproducts gradually results in a considerable increase in the viscosity of the blends. This is mainly due to the restriction of the mobility of the TPS channels.

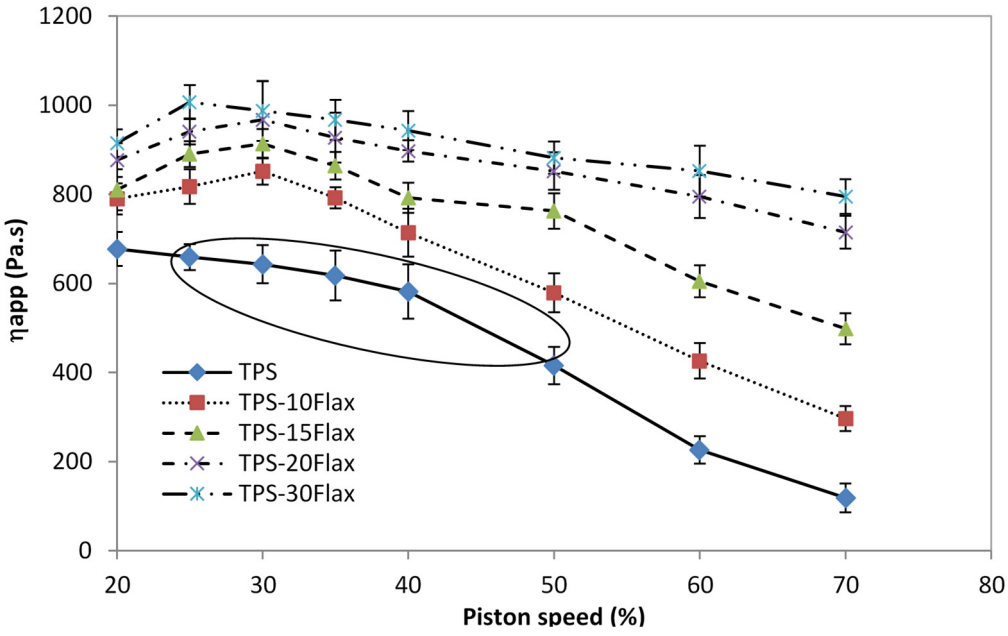

Figure 7. Variation in the apparent viscosity of the TPS/flax shives mixtures (% percentage) as a function of the shear rate (temperature 145 °C).

We also note that above 40% speed, the viscosity tends to drop very quickly up to 15% flax and very slowly for 20% and 30% flax. This difference in flow properties is strongly dependent on the state of dispersion of the flax shives and obviously, increasing the aggregate content limits the mobility of macromolecular chains and decreases the free volume, which explains the result. In order to properly homogenize the mixtures, it would be wise to act on the number of mixing cycles to homogenize the mixtures and ensure good dispersion of the plant additives while ensuring the non-degradation of the polymer. Indeed, we noticed that a partial degradation of the mixture can take place mainly at high mixing cycles (from 12 cycles).

From these findings, we decided to use an extrusion screw speed set at 50% and a cycle number set at five for the formulation of starch-based mixtures.

3.4. Evolution of the Microstructure of Biobased Mixtures

Figure 8 shows the XRD spectrum of native starch and plasticized starch. For native starch, we note that the main diffraction peaks appear at different positions (2θ = 15.2°, 17.2°, 18.1°, 20.1°, and 23.1°). Therefore, and according to Kawabata [18], we can deduce that the native starch has a type A crystal structure. This result seems quite logical since it is a starch of the cereal type. For the TPS, it can also be observed that, under the combined action of the thermomechanical treatment and the plasticizer, the profile of the diffractogram is completely different from that obtained for the native starch. We mainly note the appearance of new diffraction peaks, (2θ = 7°, 12°, 13.5°, and 18.5°) and consequently, an evolution of the type A crystal structure for native starch to an Eh/Vh type structure for plasticized starch. This confirms that the destructuring of the starch took place due to the strong shear exerted by the pistons of the RMX on the material. It should be noted that the Eh structure is slightly stable and is likely to evolve over time to transform into a type Vh structure [27].

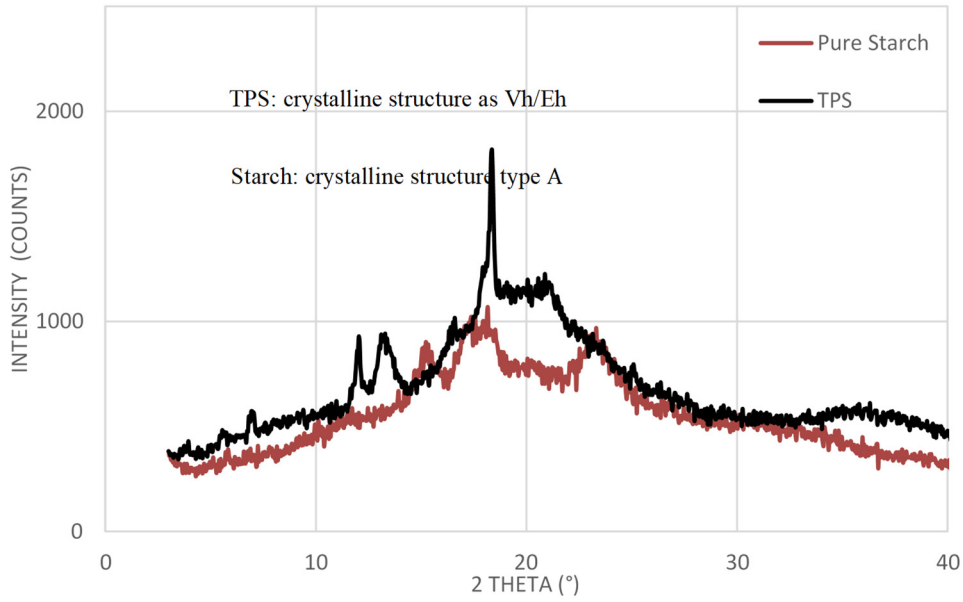

Figure 8. Standardized XRD spectrum of native starch and TPS plasticized starch.

However, the addition of flax fibers, especially in high proportions, seems to affect the microstructure of the plasticized starch (Figure 9). Indeed, it seems that the intensity of the peaks (2θ = 15.2°, 17.2°, 18.1°, and 20.1°) tends to increase. These variations may be indicative of a change in the crystalline microstructure of plasticized starch-based biocomposites. Similar observations have been reported for plasticized starch based on cellulose fibers [18] and based on jute and kapok fibers [20] and the crystallinity of these

mixtures markedly increased. However, for TPS-10Flax, the DRX spectrum appears to be unchanged and hence the crystallinity of the plasticized starch as well.

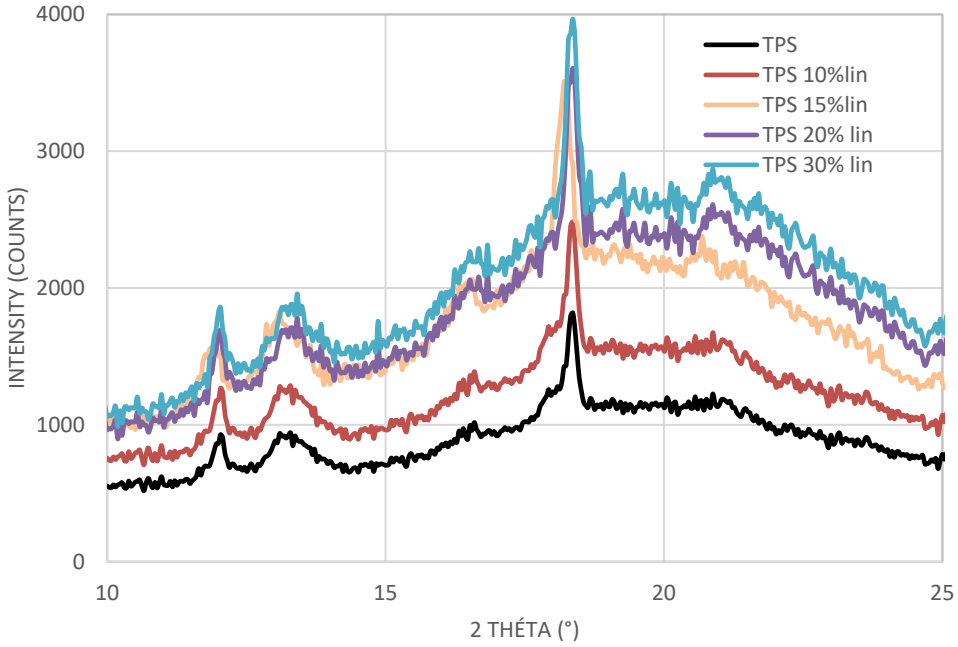

Figure 9. Normalized DRX spectrum of TPS/(% percentage) shives of flax mixtures.

3.5. Evaluation of Thermogravimetric Properties

Figure 10 shows the mass change profile of native starch and plasticized starch. We can clearly identify two phases of mass loss. The first phase is attributed to the evaporation of water and glycerol [18,19] which starts from 100 °C. In this phase, the percentage of mass loss is 11% and depends, generally, on the moisture content present in the samples. The second phase of mass loss represents the thermal decomposition of starch, which begins at around T_{onset} = 240 °C before being fully decomposed at 300 °C. From these thermograms, it appears that the mixing process (RMX) has no direct effect on the degradation temperature of the plasticized starch.

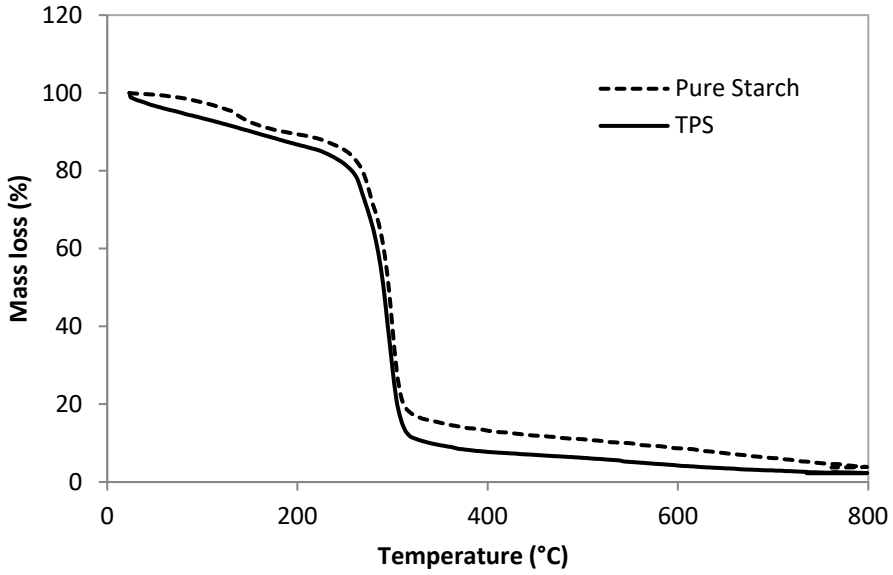

Figure 10. Thermogravimetry analysis (TGA) for native starch and TPS.

For biocomposite materials and more particularly those with low proportions of flax (10 and 15%), the profile of the mass loss thermograms (Figure 11) is similar to that obtained for the TPS and the decomposition temperature remains almost unchanged. On the other hand, at high proportions of flax (20 and 30%), there is a slight increase in the decomposition temperature (inflection point) of the plasticized starch/linseed shives mixtures and consequently the thermal stability of the biocomposite TPS/flax shives is improved. This result can be explained by the presence of lignin which is characterized by excellent thermal properties (lignin degradation temperature of around 450 °C).

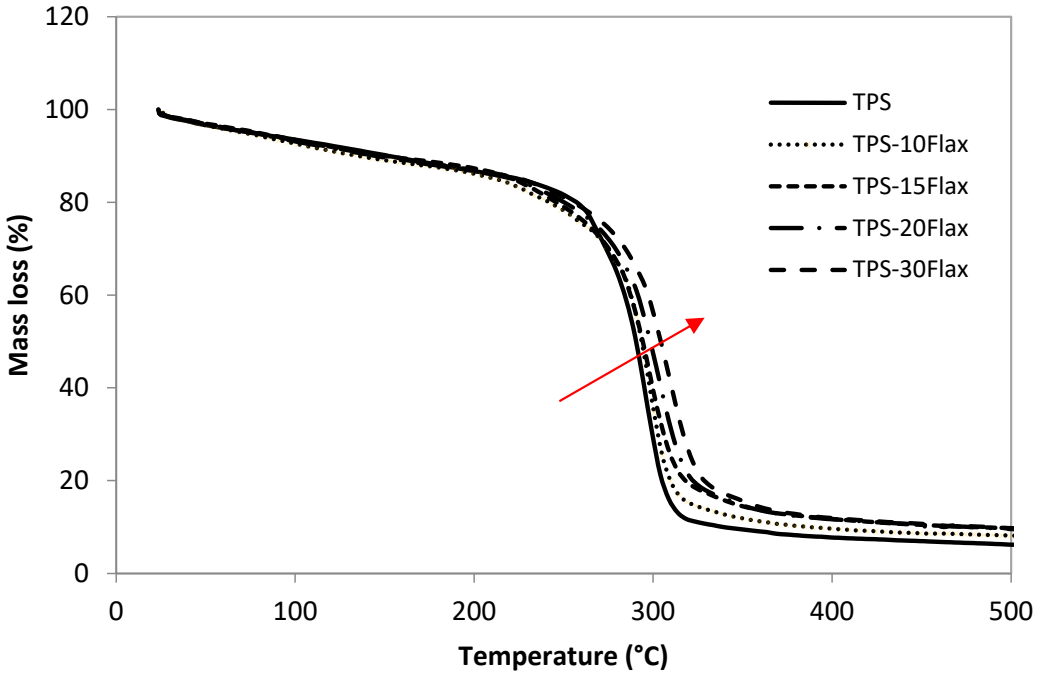

Figure 11. Thermograms (ATG) of mass loss of plasticized starch mixtures (TPS)/(% percentage) flax shives.

3.6. Assessment of Viscoelastic Properties

Thermomechanical analysis is widely used to determine the variation in mechanical properties with temperature. The elastic modulus E′ is representative of the stiffness of materials and the tan δ factor provides us information on the relaxations of the polymer [34].

Figure 12 shows the variation in the storage modulus (E′) of plasticized starch (TPS) and TPS/flax shives as a function of temperature. On this graph, there are three zones: glassy zone (20 to 45 °C), glass transition zone (40 to 80 °C), and the rubbery zone (above 80 °C). Note that the storage modulus (E′) of TPS gradually decreases with increasing temperature. However, the addition of flax shives contributes to improving the viscoelastic behavior in the glassy domain; therefore, the stiffness of the biocomposite mixtures is higher than that of TPS. The positive effect of flax shives is clearly identified in the vitreous region (20 to 80 °C). Above 80 °C, the contribution of flax shives is less visible and the storage modulus (E′) of the biocomposites are greatly influenced by the softening of the polymer.

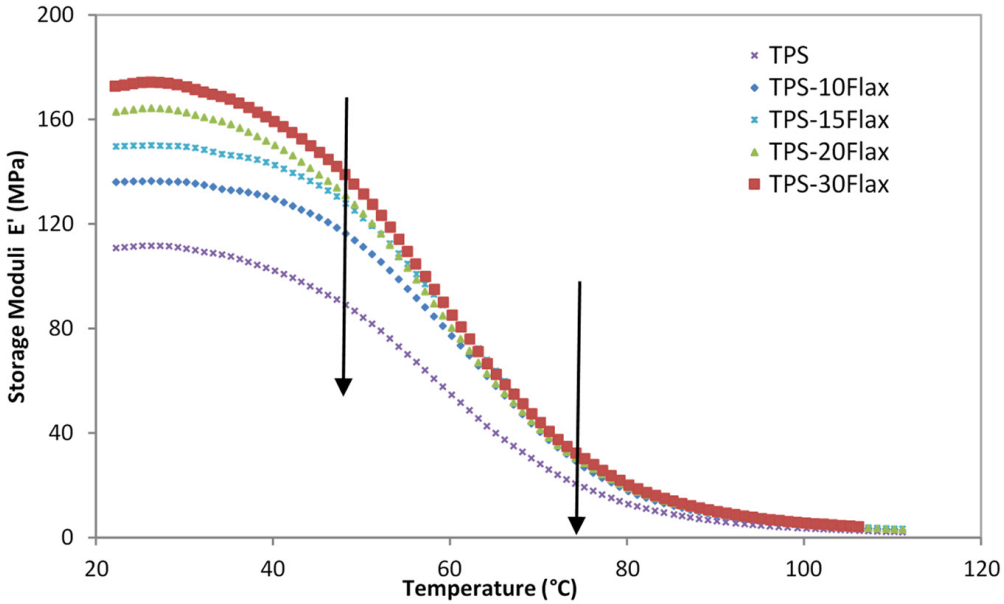

Figure 12. Evolution of the storage modulus E′ for TPS and TPS/(% percentage) shives of flax as a function of temperature.

We also note, for the TPS, a main relaxation at T = 82 °C which corresponds to the glass transition temperature (Figure 13). Similar observations have also been reported [35–37]. However, the addition of flax shives causes a decrease in the intensity of the tan δ peak and a very slight shift of the glass transition temperature towards higher values. This is even more observed with high proportions of flax shives (30%).

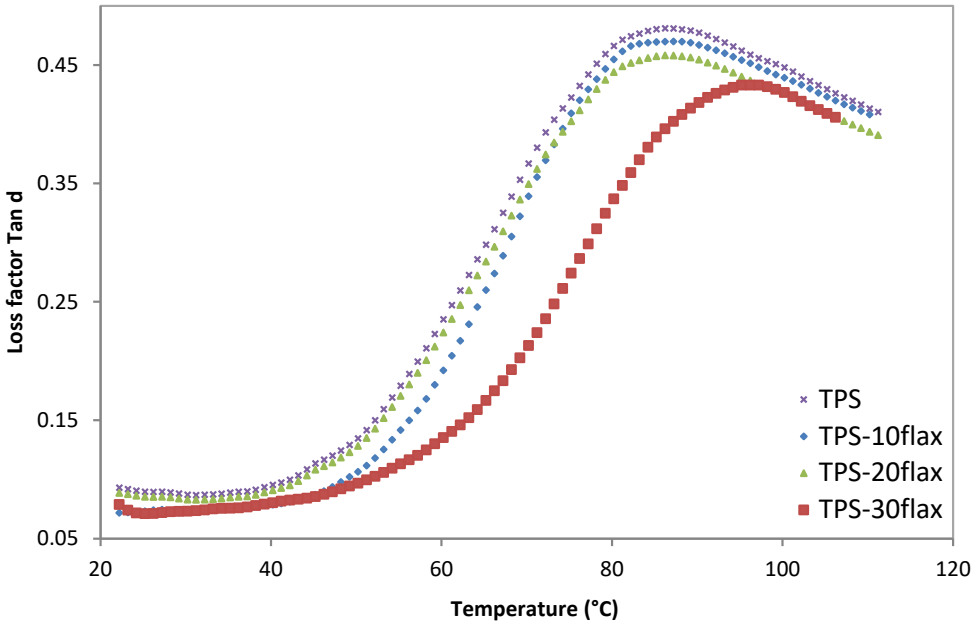

Figure 13. Evolution of the tan δ factor for TPS and TPS/(% percentage) shives of flax as a function of temperature.

These observations can be explained by the reduction in polymer chain mobility caused by the intermolecular interactions between flax aggregates and TPS. Indeed, these interactions can be explained by a nucleating effect which promotes the rapid crystallization of TPS. It can be also attributed to a slight lamellar sliding and rotation in the crystalline zone of the TPS. We note a shift in the band of the peak tan δ, at 30% flax shives, which can correspond to a lamellar movement of the crystalline zone, which is more affected by the presence of flax shives.

4. Discussion

The formulation of TPS starch filled with flax shives is mainly governed by the RMX parameters process, particularly the number of cycle mixing and internal shearing.

The apparent viscosity of molten mixtures decreased significantly as the shearing phenomenon is more pronounced. Six mixing cycles is the optimal compromise for a stable apparent viscosity. This also reflected a better homogeneity of the different fraction's synonyms of the suitable processability of the different mixtures. The shearing rate (piston speed) significantly affected the rheological behavior. A good compromise was found at a speed rate of 50% and allows a good processability and rearrangement of the different internal fraction. We should mention that at a low or high-speed rate, we can rush the thermal degradation of TPS mixtures. As reported, TPS is very sensitive to humidity and temperature and its internal structure can weaken if the transformation conditions are not well-chosen. The addition of flax shives contributes to improving the viscoelastic behavior in the glassy domain (Tg near 90°), the biocomposites stiffness is higher in this glassy region. However, for higher temperature the softening of TPS dominated the whole viscoelastic behavior od TPS/flax mixtures and the reinforcement effect of flaw is attenuated. From a microstructural point of view, the findings show that the starch TPS exhibits crystal structures of Eh and Vh types compared with a crystal structure of type A, for native starch, which is predominantly amorphous. The evolution of starch crystallinity can come from a new macromolecular rearrangement and probably the formation of amylose and lipid complexes due to elongational flow, high shear, and the presence of flax shives which can favor the formation of crystalline spherulites at the TPS/flax shives interface. Furthermore, the thermal stability of TPS is more improved by the addition of flax shives, probably attributed to the lignin fraction present in flax shives, which has excellent thermal properties.

5. Conclusions

The objective of this study is potentially to better formulate biobased starch-based mixtures. The RMX thermomechanical mixer was used as an innovative concept which favors elongational flow. It contributes greatly to increasing the efficiency of the dispersion mechanisms of multiphase mixtures and allows the development and the direct measurement of their rheological properties. According to our methodology, a shearing rate of (50%) and cycle mixing number (6) are the suitable parameters to mix a TPS/flax mixture. The rheological and viscoelastic analysis were carried out and show a direct effect of the last parameters on the processability of these mixtures. High stiffness behavior of TPS was observed in the glassy region, as well as a good dispersion of both phase (TPS) and flax. The crystalline phase of TPS was affected according to both by RMX shearing and flax addition. Furthermore, the thermal stability of TPS was improved by the addition of flax shives. Other experiments should be performed on the mechanical performance, humidity adsorption, and biodegradability of TPS/flax-based materials.

Author Contributions: M.R.: Conceptualization, Methodology, Experimentations, Data curation, Validation, Formal analysis, Writing—Original draft preparation, Review & editing. C.T. and N.L.: Funding acquisition, visualization, Review & editing, Supervision, and Project administration. All authors have read and agreed to the published version of the manuscript.

Funding: Funding from Normandy region (project reference D14-13117).

Institutional Review Board Statement: Not applicable.

Acknowledgments: The authors thank particularly the Normandy region for their financial support (BATMATOP project D14-13117).

Conflicts of Interest: The authors declare no conflict of interest.

References

1. Mohanty, A.K.; Misra, M.; Drzal, L.T. Sustainable bio-composites from renewable resources: Opportunities and challenges in the green materials world. *Polym. Environ.* **2002**, *10*, 19–26. [CrossRef]
2. Yu, L.; Dean, K.; Li, L. Polymer blends and composites from renewable resources. *Prog. Polym. Sci.* **2006**, *31*, 576–602. [CrossRef]
3. Mittal, V.; Chaudhry, A.U.; Matsko, N.B. "True" biocomposites with biopolyesters and date seed powder: Mechanical, thermal, and degradation properties. *Appl. Polym. Sci.* **2014**, *131*, 40816. [CrossRef]
4. Iannace, S.; Ali, R.; Nicolais, L. Effect of processing conditions on dimensions of sisal fibers in thermoplastic biodegradable composites. *Appl. Polym. Sci.* **2001**, *79*, 1084–1091. [CrossRef]
5. Averous, L.; Halley, P.J. Biocomposites based on plasticized starch. *Biofuels Bioprod. Biorefining* **2009**, *3*, 329–343. [CrossRef]
6. Bénézet, J.C.; Stanojlovic-Davidovic, A.; Bergeret, A.; Ferry, L.; Crespy, A. Mechanical and physical properties of expanded starch, reinforced by natural fibres. *Ind. Crop. Prod.* **2012**, *37*, 435–440. [CrossRef]
7. De Graaf, R.A.; Karman, A.P.; Janssen, L.P.B.M. Material properties and glass transition temperatures of different thermoplastic starches after extrusion processing. *Starch Staerke* **2003**, *55*, 80–86. [CrossRef]
8. Demirgoz, D.; Elvira, C.; Mano, J.F.; Cunha, A.M.; Piskin, E.; Reis, R.L. Chemical modification of starch based biodegradable polymeric blends: Effects on water uptake, degradation behaviour and mechanical properties. *Polym. Degrad. Stab.* **2000**, *70*, 161–170. [CrossRef]
9. Haroon, M.; Wang, L.; Yu, H.; Abbasi, N.M.; Zain-ul-Abdin, Z.-A.; Saleem, M.; Khan, R.U.; Ullah, R.S.; Chen, Q.; Wu, J. Chemical modification of starch and its application as an adsorbent material. *RSC Adv.* **2016**, *6*, 78264–78285. [CrossRef]
10. Ayoub, A.S.; Rizvi, S.S.H. An overview on the technology of cross-linking of starch for nonfood applications. *J. Plast. Film. Sheet* **2009**, *25*, 25–45. [CrossRef]
11. Ke, T.; Sun, X. Thermal and mechanical properties of poly(lactic acid) and starch blends with various plasticizers. *Trans. Am. Soc. Agric. Eng.* **2001**, *44*, 945–953.
12. Pyshpadass, H.A.; Marx, D.B.; Hanna, M.A. Effects of extrusion temperature and plasticizers on the physical and functional properties of starch films. *Starch Staerke* **2008**, *60*, 527–538. [CrossRef]
13. Shi, R.; Zhang, Z.; Liu, Q.; Han, Y.; Zhang, L.; Chen, D.; Tian, W. Characterization of citric acid/glycerol co-plasticized thermoplastic starch prepared by melt blending. *Carbohydr. Polym.* **2007**, *69*, 748–755. [CrossRef]
14. Talja, R.A.; Helen, H.; Roos, Y.H.; Jouppila, K. Effect of various polyols and polyol contents on physical and mechanical properties of potato starch-based films. *Carbohydr. Polym.* **2007**, *67*, 288–295. [CrossRef]
15. Gao, W.; Wu, W.; Liu, P.; Hou, H.; Li, X.; Cui, B. Preparation and evaluation of hydrophobic biodegradable films made from corn/octenylsuccinated starch incorporated with different concentrations of soybean oil. *Int. J. Biol. Macromol.* **2020**, *142*, 376–383. [CrossRef]
16. Bulkin, B.J.; Kawak, Y. Retrogradation kinetics of waxy-corn and potato starches: A rapid, Raman-spectroscopic study. *Carbohydr. Res.* **1987**, *160*, 95–112. [CrossRef]
17. Gudmundsson, M. Retrogradation of starch and the role of its components. *Thermochim. Acta* **1994**, *246*, 329–341. [CrossRef]
18. Liu, Q.; Thompson, D.B. Effects of moisture content and different gelatinization heating temperatures on retrogradation of waxy-type maize starches. *Carbohydr. Res.* **1998**, *314*, 221–235. [CrossRef]
19. Dammak, M.; Fourati, Y.; Tarrés, Q.; Delgado-Aguilar, M.; Mutje, P.; Boufi, S. Blends of PBAT with plasticized starch for packaging applications: Mechanical properties, rheological behaviour and biodegradability. *Ind. Crop. Prod.* **2020**, *144*, 112061. [CrossRef]
20. Palai, B.; Biswal, M.; Mohanty, S.; Nayak, S.K. In situ reactive compatibilization of polylactic acid (PLA) and thermoplastic starch (TPS) blends; synthesis and evaluation of extrusion blown films thereof. *Ind. Crop. Prod.* **2019**, *141*, 11174. [CrossRef]
21. Dang, K.M.; Yoksan, R.; Ollet, P.E.; Avérous, L. Morphology and properties of thermoplastic starch blended with biodegradable polyester and filled with halloysite nanoclay. *Carbohydr. Polym.* **2020**, *242*, 116392. [CrossRef]
22. Dufresne, A.; Vignon, M.R. Improvement of starch film performances using cellulose microfibrils. *Macromolecules* **1998**, *31*, 2693–2696. [CrossRef]
23. Dufresne, A. Dynamic mechanical analysis of the interphase in bacterial polyester/cellulose whiskers natural composites. *Compos. Interfaces* **2000**, *7*, 53–67. [CrossRef]
24. Funke, U.; Bergthaller, W.; Lindhauer, M.G. Processing and characterization of biodegradable products based on starch. *Polym. Degrad. Stab.* **1998**, *59*, 293–296. [CrossRef]
25. Curvelo, A.; Carvalhoa, A.J.F.; Agnellib, J.A.M. Thermoplastic starch–cellulosic fibers composites: Preliminary results. *Carbohydr. Polym.* **2001**, *45*, 183–188. [CrossRef]
26. Tokihisa, M.; Yakemoto, K.; Sakai, T.; Utracki, L.A.; Sepehr, M.; Li JSimard, Y. Extensional flow mixer for polymer nanocomposites. *Polym. Eng. Sci.* **2006**, *46*, 1040–1050. [CrossRef]

27. VanSoest, J.J.G.; De Wit, D.; Vliegenthart, J.F.G. Mechanical properties of thermoplastic waxy maize starch. *Appl. Polym. Sci.* **1996**, *11*, 1927–1937. [CrossRef]
28. Mikus, P.Y.; Alix, S.; Lacrampe, M.F.; Krawczak, P.; Coquerel, X.; Dole, P. Deformation mechanisms of plasticized starch materials. *Carbohydr. Polym.* **2014**, *114*, 450–457. [CrossRef]
29. Fengwei, X.; Peter, J.H.; Luc, A. Rheology to understand and optimize processibility, structures and properties of starch polymeric materials. *Prog. Polym. Sci.* **2012**, *37*, 595–623.
30. Martin, O.; Averous, L.; Della Valle, G. In-line determination of plasticized wheat starch viscoelastic behavior. *Carbohydr. Polym.* **2003**, *53*, 169–182. [CrossRef]
31. Muller, R.; Bouquey, M.; Abbas, L.; Triki, B. Un nouveau type de mélangeur: Réalisation d'un prototype et premiers résultats. *Rhéologie* **2007**, *12*, 27–36.
32. Mahieu, A.; Alix, S.; Leblanc, N. Properties of particleboards made of agricultural by-products with a classical binder or self-bound. *Ind. Crop. Prod.* **2019**, *130*, 371–379. [CrossRef]
33. Arufe, S.; Hellouin de Menibus, A.; Leblanc, N.; Lenormand, H. Physico-chemical characterisation of plant particles with potential to produce biobased building materials. *Ind. Crop. Prod.* **2021**, *171*, 113901. [CrossRef]
34. Kawabata, A.; Sawayama, S.; Nagashima, N.; Nakamura, M. *Journal of the Japanese Society of Starch Science*; The Japanese Society of Applied Glycoscience: Tokyo, Japan, 1984; Volume 31, pp. 224–232.
35. Kim, H.S.; Yang, H.S.; Kim, H.J.; Lee, B.J.; Hwang, T.S. Thermal properties of agro flour filled biodegradable polymer bio composites. *J. Therm. Anal. Calorim.* **2005**, *81*, 299–306. [CrossRef]
36. Belhassen, R.; Boufi, S.; Vilaseca, F.; López, J.P.; Méndez, J.A.; Franco, E.; Pèlach, M.A.; Mutjé, P. Biocomposites based on Alfa fibers and starch-based biopolymer. *Polym. Adv. Technol.* **2009**, *20*, 1068–1075. [CrossRef]
37. Famá, L.; Gerschensonb, L.; Goyanesa, S. Starch vegetable fibre composites to protect food products. *Carbohydr. Polym.* **2009**, *76*, 230–235. [CrossRef]